2016

# The Effect of pH on the Photoluminescent Properties of Silicon Nanoparticles

Parker Karaba
*Portland State University*

# The Effect of pH on the Photoluminescent Properties of Silicon Nanoparticles

By

Parker Karaba

An undergraduate honors thesis submitted in partial fulfillment of the

requirements for the degree of

Bachelor of Science

in

University Honors

and

Chemistry

Thesis Adviser

Dr. Andrea Goforth

Portland State University

2016

Abstract:

Since the discovery of photoluminescent (PL) emissions from nanosilicon in 1990, there has been an increased effort to understand this phenomenon, as well as applications it might serve. In particular, the potential use of silicon nanoparticles (SiNPs) in the biomedical industry as optical contrast agents has garnered attention due to the non-toxicity of silicon, as well as its abundance and low cost. It is therefore prudent to understand factors that effect the PL behavior of these SiNPs in biological media. In this research, hydrogen terminated SiNPs (H-SiNPs) were synthesized using a sol-gel method, suspended in ethanol, then titrated with aqueous acid and base. The resulting behavior was then characterized with Fourier-transform infrared and photoluminescence emission and excitation spectroscopies. It was observed that suspension of red emitting H-SiNPs ($\lambda_{max,em}$ ~630 nm) in ethanol led to a quenching of PL emissions and a reduction of hydrogen termination on their surface. Titration of the ethanol suspension with acid led to a resurgence of the red emissions, while titration with base did not induce any observable PL emissions. Additional modification by warming and resuspension into hexane also led to a brief resurgence of the red emissions in both cases. While the work presented here is relatively focused in scope, it raises a number of questions regarding the structure and behavior of SiNPs for future exploration and research.

Table of Contents

Table of Figures

Introduction:

*1.1 Nanoparticles: History and Applications*

Nanoparticles (NPs), particles with a diameter within the range of 1-100 nanometers, have a rich history and are used in a variety of applications in modern society due to their unique optical and electronic properties. The term nanoparticle encompasses a wide variety of different organic materials, including proteins and polysaccharides, as well as inorganic materials, such as iron oxyhydroxide and aluminosilicate NPs.

Historically, many of these NPs were employed as dyes and paints, due to their unique metallic luster and iridescent qualities. Such applications can be traced back to as early as the 4$^{th}$ century, when gold NPs were used to paint glass red, as seen in the Roman Lycurgus cup (Figure 1). Silver and copper NPs were used in ceramic glazes and paints in 9$^{th}$ century Mesopotamia. The spacing of the NPs in these glazes resulted in unique optical interference, causing light scattering and specular reflection visible on their surfaces. Meaningful attempts to understand NPs and their optical properties began in earnest in the 1800s, when colloidal gold NPs were synthesized from sodium tetrachloroaurate ($Na[AuCl_4]$).[1]

Since then, NP research has dramatically expanded to examine other materials for applications of NPs. While metallic NPs are still relevant in contemporary research, there has been an increased focus on semiconductor NPs, which will be the focus of the research discussed herein; specifically, silicon. Semiconductor NPs possess unique optical and electronic properties, such as stable, tunable photoluminescence (PL) and electroluminescence (EL), which they do not possess when in the bulk state.[2] Such properties have made these NPs applicable in areas such as optoelectronics, photovoltaics and catalysis.[1-4]

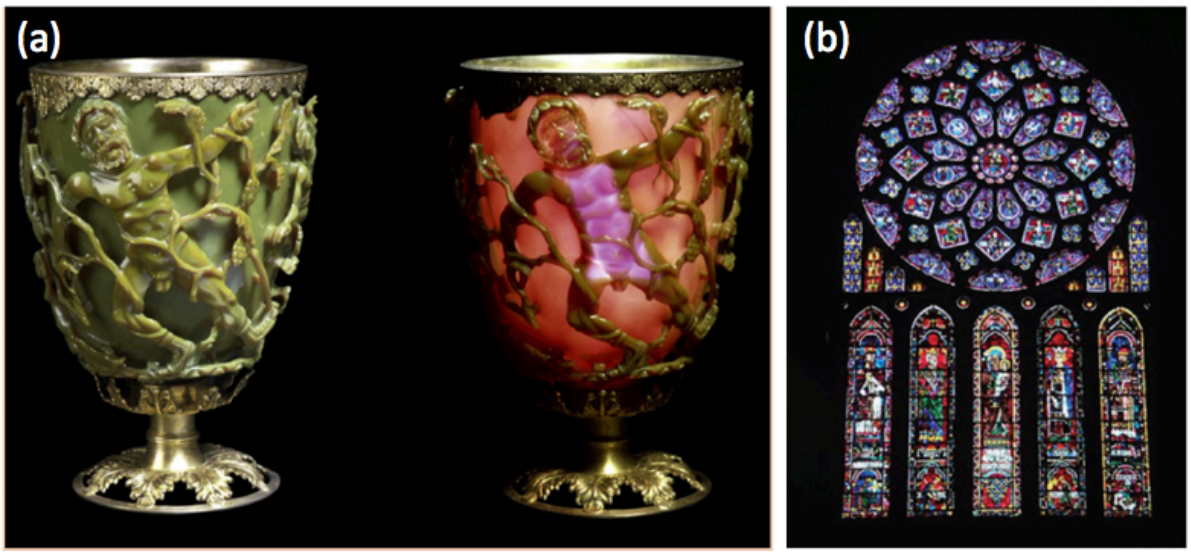


Figure 1: Applications of NP colloids as dyes and paints. (a) The Lycurgus cup, a 4th century artifact manufactured by the Romans painted with a gold and silver NP colloid that changes from green to red depending on the location of illumination. (b) A stained glass window within the Chartres Cathedral, constructed in the 13th century and painted with a silver NP suspension.[1]

*1.2 Nanoparticles: Mechanism of Action*

The unique optical and electronic properties of SiNPs are primarily the result of the quantum confinement (QC) effect, which gives rise to a dependency between particle size and band gap energy. Within bulk semiconductors, electrons are able to move within a continuum of occupied energy levels, referred to as the valence band (VB). The VB is energetically separated from a continuum of vacant energy levels, known as the conduction band (CB). Electrons in the VB can be promoted to the CB as a result of energy being added into the system (electrical, light, heat, etc.), leaving oppositely charged "electron holes" in their place.[5] In doing so, they cross the band gap, a non-occupied region between the VB and CB, which also represents the energy difference between the two bands. In semiconductor materials, the band gap can either exist as direct or indirect (Figure 2). In a direct band gap semiconductor, the minimum of the CB and the maximum of the VB exist with the same momentum. This means that an electron-hole pair can form more easily with less energy input, and can also recombine without the need to lose excess

energy, as they possess they same momentum. An indirect band gap material is one in which the minimum energy level of the CB and maximum energy level of the VB do not exist with the same momentum, and are out of phase. Thus, for electrons to be promoted to the CB, they require both an input of energy to cross the band gap and to change their momentum; this is also true for recombination.[6,7] As a result, indirect band gap semiconductors require more energy to generate PL emissions, and as a result, are typically slower and less efficient.[6,8]

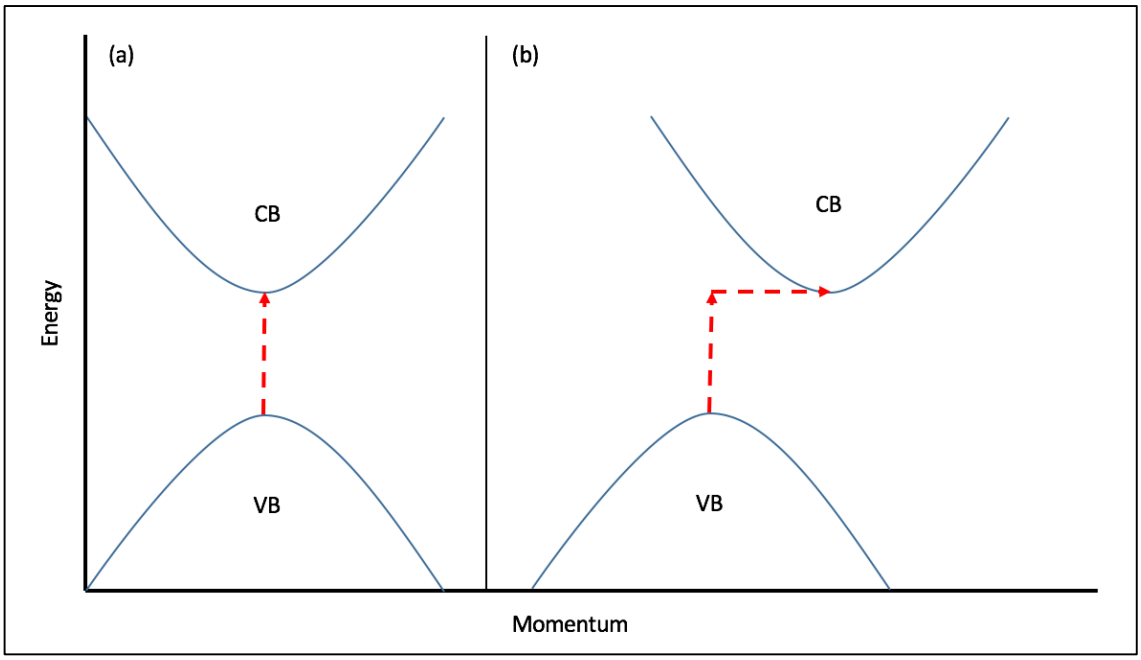


Figure 2: Energy band diagram comparing direct band gap (a) and indirect band gap (b) semiconductors. While both semiconductors require an input of energy to excite an electron from the VB to the CB, the indirect band gap semiconductor also requires a change in momentum.

The separation of the electron and electron hole (together, called an exciton) results in the formation of current, a product of the electron and electron hole freely traversing the material. This is a property harvested in modern semiconductor devices and commonly seen in bulk materials resulting from the absence of spatial confinement exerted upon the exciton, thus allowing the electron and electron hole to overcome their electrostatic attraction. When the bulk semiconductor

diameter is decreased such that it is spatially confined in one or more dimensions, the exciton becomes confined and its movement constrained. When the exciton is constrained in one dimension, the result is referred to as a quantum well; constraint in two dimensions is a quantum wire; constraint in three dimensions is a quantum dot (QD). This leads to the emergence of quantum effects and a breakdown of 'classical physics'. As a result, in a semiconductor QD the electron hole and electron are forced to recombine, which can lead to radiative emission. In addition, as the NP becomes dimensionally confined, the density of states at the band edges decreases, resulting in a breakdown of the energy continuum around the band gap and an increase in the overall gap energy. Thus, as the particle continues to decrease in size, size-dependent emission arises, and the PL energy can be tuned as such. This size effect can be quantified with the Brus equation,

$$E_{g(QD)} = E_{Bulk} + \frac{h^2}{8R^2}\left(\frac{1}{m_e^*} + \frac{1}{m_h^*}\right) \quad (1)$$

, where $E_{g(QD)}$ is the band gap energy of the quantum dot (QD), $E_{Bulk}$ is the band gap energy of the bulk semiconductor, h is Planck's constant, R is the radius of the quantum dot, $m_e^*$ is the effective mass of the excited electron, and $m_h^*$ is the effective mass of the excited electron hole.[9] The effect was first shown experimentally in the 1980s with CdS NPs.[1] In general, the behavior of direct band gap semiconductor NPs, such as CdSe and PbS NPs is in good agreement with the QC model.

*1.3 Other Mechanisms of Photoluminescence*

Even though QC is often acknowledged as one of the primary causes for the characteristic PL, other factors, such as shape, composition, density, and surface alteration can influence this mechanism. In direct band gap semiconductor NPs, such as those composed of heavy metals, the PL emissions strongly correlate with particle size and are in good agreement with the predictions made by the QC model, indicating that it is the predominating radiative mechanism. This is demonstrated in a number of reports, such as one by Wang et. al, in which size-controlled CdSe quantum dots were synthesized and demonstrated a strong correlation to the predicted PL energy.[10] However, this is not always the case with indirect band gap semiconductor NPs, such as SiNPs.

Many studies of SiNP emissions focus on hydrogen passivated SiNPs (H-SiNPs), and typically, the experimental data of particle size and emission wavelength of H-SiNPs are in good agreement with those predicted by the quantum mechanical model. However, there are a number of instances in which deviations from the QC model can be seen among SiNPs. As reported by Fuzell et. al, SiNPs prepared under different synthetic protocols but under identical ambient conditions yielded both blue and red emissions. They postulated this discrepancy to be the result of the presence of low-density traps from nitrogen impurities on the surface of the NPs.[11] Other reports have indicated that non-QC PL emissions may be the result of differences between the radiative mechanisms of direct and indirect band gap semiconductors, as well as the presence of surface traps.[7,8,12-14]

The presence of functional groups on the surfaces of such NPs has also been empirically shown to cause non-QC PL emissions, but the mechanism responsible for these emissions is not entirely known. In a study reported by Dasog et al., the presence of functional groups was shown to allow for the modification of SiNPs PL across the visible spectrum (Figure 3). In the study,

dodecylamine, diphenylamine, and trioctylphosphine oxide caused SiNPs to fluoresce blue, green and yellow, respectively.[15] Knittel et al. demonstrate that the presence of surface defects can have adverse effects on the wavelength of photoluminescence, demonstrated by the capping of SiNPs with tritiated oleic acid.[16] Surface oxidation has also been shown to modify the PL energy of SiNPs. Such oxidation can occur upon exposure to air due to the propensity of silicon to react with oxygen, resulting in the formation of a silicon oxide shell around the core of the NPs. Additionally, depending on the synthetic strategy utilized to generate the SiNPs, this oxidation has been experimentally shown to generate both red-shifted and blue-shifted emissions, further highlighting the complexity of this oxidative reaction, and the photoluminescence mechanism.[17-23]

Figure 3: SiNPs functionalized with various surface groups. The functional groups, from left to right: dodecylamine, acetal, diphenylamine, TOPO, dodecyl (air), dodecyl (inert). From [15]

However, such oxidation is not exclusive to air, as surface oxidation and other unique interactions can occur between SiNPs and aqueous acid and base. As demonstrated by Chiu et al., SiNP PL can be modified by titration of the colloids with either acid or base. In their study, SiNPs in acidic solutions exhibited strong red PL, while those in basic solution exhibited strong blue PL. Furthermore, it was also found that the pH of the colloid could be adjusted in either direction to

convert PL from red to blue, or *vice versa*. The mechanism for PL switching was hypothesized to be due to the changing surface chemistry of the NPs.[24] Further analysis is required to fully understand the mechanism.

*1.4 Silicon Nanoparticles: A Cut Above*

Heavy-metal, direct band gap NPs have found an especially increased utility in biomedical applications as optical contrast agents, and their size and tunable PL also make them useful for drug delivery, diagnostic procedures and fluorescent imaging.[25] However, the toxicity of heavy metal nanoparticles makes their use in biological applications unsafe. For example, cadmium containing NPs have been linked to altered cell growth and damaged DNA.[26] Therefore, SiNPs are being increasingly studied for these applications due to the low toxicity of Si, as well as its high relative abundance. Additionally, the theoretical tunability of PL energy gives SiNPs an advantage over molecular fluorophores commonly used in medicine such as rhodamine, fluorescein, and phycoerythrin.[25]

Bulk silicon has long been used in modern electronics. However, it was not until 1990, when it was discovered that the UV excitation of silicon wafers following particular electrochemical etching procedures resulted in red-orange PL, that interest in nanocrystalline silicon began to grow.[1,2] This discovery led to further investigation into the properties of porous and thin film silicon structures, which revealed its propensity towards surface functionalization, relative stability against photochemical alteration, and its nontoxicity, making it especially desirable for use in nanochemistry over similar, heavy-metal based NPs. Now, silicon is a ubiquitous material used in nanochemistry, and SiNPs are frequently employed as components in solar cell batteries, photocatalysts, and in light emitting diodes (LEDs).[2]

There are currently a number of synthetic strategies employed to synthesize SiNPs, which can be divided into two categories: top-down and bottom-up approaches. Common top-down approaches, which start from bulk materials and breaks them down to the nanoscale, include pulsed laser ablation (PLA) of silicon wafers, ball milling of silicon dioxide followed by annealing and photothermal aerosol synthesis. Bottom-up approaches, which involve the assembly of NPs from smaller components, include thermolysis, pyrolysis, and chemical synthesis using a variety of precursors, such as silicon halides and Zintl salts.[2,3]

*1.5 HSiNP Synthesis from $SiO_{1.5}$ Polymer*

One such bottom-up synthetic method is described by Henderson et al., and a modified version of this process will be employed in this research.[27] The process first involves the reaction between trichlorosilane and water, resulting in a hydrolysis reaction following a nucleophilic attack by water at the silicon center. This induces the breaking of the Si-Cl bond, and the formation of an Si-OH bond. Following this, a condensation reaction occurs and results in a covalent linkage between silicon and oxygen, called a 'siloxane' linkage. Finally, this condensation reaction is polymerized for each silicon linkage, forming a complex three-dimensional matrix of silicon and oxygen, with putative Si:O stoichiometry of 1:1.5 (Figure 4a).[27-29] This is followed with thermal processing at $1100^0$C, which results in the redistribution of silicon throughout the oxide matrix, leading to clustering and the formation of silicon domains embedded within a matrix composed of silicon dioxide (Figure 4b).[27,30]

This is followed by the etching of the annealed polymer by a hydrofluoric acid solution. HF possesses a propensity towards reacting with $SiO_2$, according to the following reaction:

$$SiO_2 + 4HF \rightarrow SiF_4 + 2H_2O$$

Thus, etching in HF results in the gradual consumption of the silicon dioxide layer of the SiNPs. The HF solution can continue to react with the silicon domains, resulting in the breaking of Si-Si bonds as seen in the following reaction:

$$Si + 4HF \rightarrow SiF_4 + 2H_2$$

The silicon on the surface of the domain then reacts with the $H^+$ in solution, forming Si-H bonds and resulting in a hydride-terminated domain (Figure 4c).[31-34]

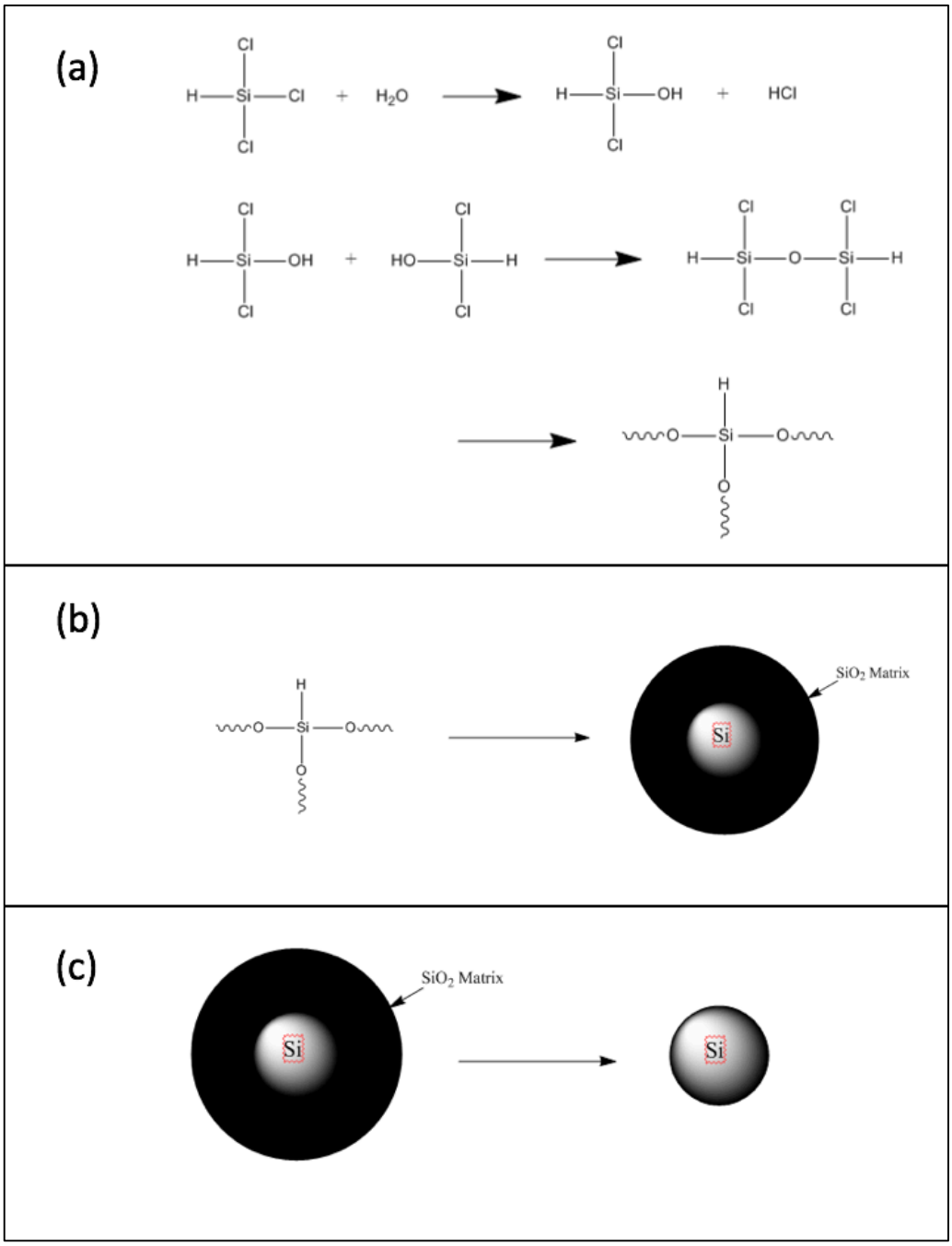


Figure 4: The reaction scheme for the H-SiNP synthetic method. (a) A polymerization reaction occurs first, in which a condensation reaction occurs following a hydrolysis reaction, forming a polymerized matrix of siloxane linkages. (b) Annealing results in the formation of silicon domains surrounded by a matrix of $SiO_2$. (c) Etching in HF results in the liberation of the Si domains from the matrix.

Experimental:

*2.1 Materials and Instrumentation:*

The following reagents and chemicals were used as received: trichlorosilane (98%, Alfa Aesar), hydrofluoric acid (49%, Sigma Aldrich), n-hexane (>95%, Acros Organics), and hydrochloric acid (12.1N, Fisher Scientific). Ethanol (95%) and potassium hydroxide pellets were obtained from the Portland State University stockroom and used without further purification.

PL emission and excitation spectroscopy measurements were both taken with a Shimadzu RF-5301 PC Spectrofluorophotometer. Fourier-transform infrared (FT-IR) spectroscopy was conducted with a ThermoFisher Scientific Nicolet iS10 FTIR, equipped with a diamond attenuated total reflectance (ATR) attachment.

*2.2 Synthesis of H-Si NPs:*

The synthesis of hydrogen terminated SiNPs was adapted from an altered literature procedure.[27] First, 5 mL of trichlorosilane ($HSiCl_3$) was injected into an argon-filled two necked round bottom flask kept at $0^0$C to prevent vaporization of the sample. Next, approximately 6 mL of nanopure water was carefully injected into the flask, and the mixture was left to magnetically stir under flowing Ar to promote completion of the reaction. If necessary, an additional 1 mL of water was also injected if liquid $HSiCl_3$ was still visible inside the flask. Upon formation of the silicon-oxide polymer, the flask was vented under flowing Ar at room temperature for 24 hours, and then at $120^0$C for an additional 24 hours to remove residual water, as well as gaseous HCl produced by the reaction.

Once dried, the resulting $HSiO_{1.5}$ polymer, was removed from the flask, where it was ground up into a fine powder. An alumina boat was then filled with the polymer, and subsequently

heated according to the following temperature profile under flowing $N_2$(g) within a Lindberg Blue M tube furnace:

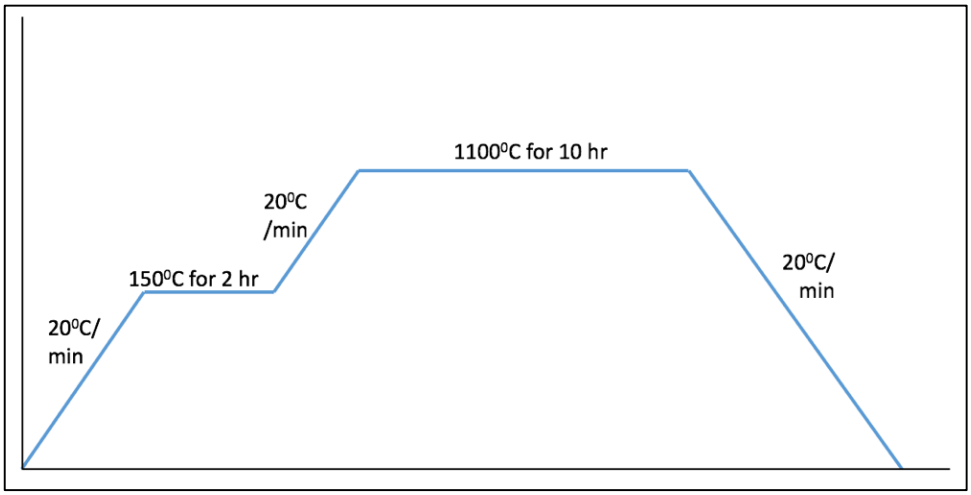


Figure 5: Temperature profile for annealing of $SiO_{1.5}$ polymer

The annealed polymer was then loaded into a stainless steel milling vial equipped with two 1 cm stainless steel balls and mechanically milled for 10 s with a Spex 8000M mixer/miller, and the milled polymer was then stored under Ar until further use. Approximately 0.50g of the milled, annealed polymer was added to a Teflon beaker. To this, 5 mL of EtOH, $H_2O$ and HF were added, and the solution was set to stir for 60 minutes. Following this, the H-SiNPs were phase-transferred from the aqueous solution into a total of 50 mL of n-hexane by a biphasic extraction. The colloid was Ar protected until further use.

*2.3 Acid/Base Titrations of SiNPs:*

The SiNPs were isolated from the hexane colloids by centrifugation at 2500 rpm for 15 minutes, and then suspended into 5mL of ethanol. The mixtures were then sonicated thoroughly to promote dispersion of the particles. Immediately following suspension in ethanol, the aliquots were individually titrated with volumes of 5, 15 and 25 µL of 12.1 N HCl and 6M KOH. Control samples of SiNPs in ethanol were monitored in tandem. Other aliquots were heated to $60^0$C for 30 minutes following suspension. Additionally, one aliquot of the SiNP/EtOH sample was centrifuged immediately after suspension, and the EtOH replaced with 5 mL of hexane to observe if PL emissions could be restored. An overview of these modifications can be seen in Figure 6.

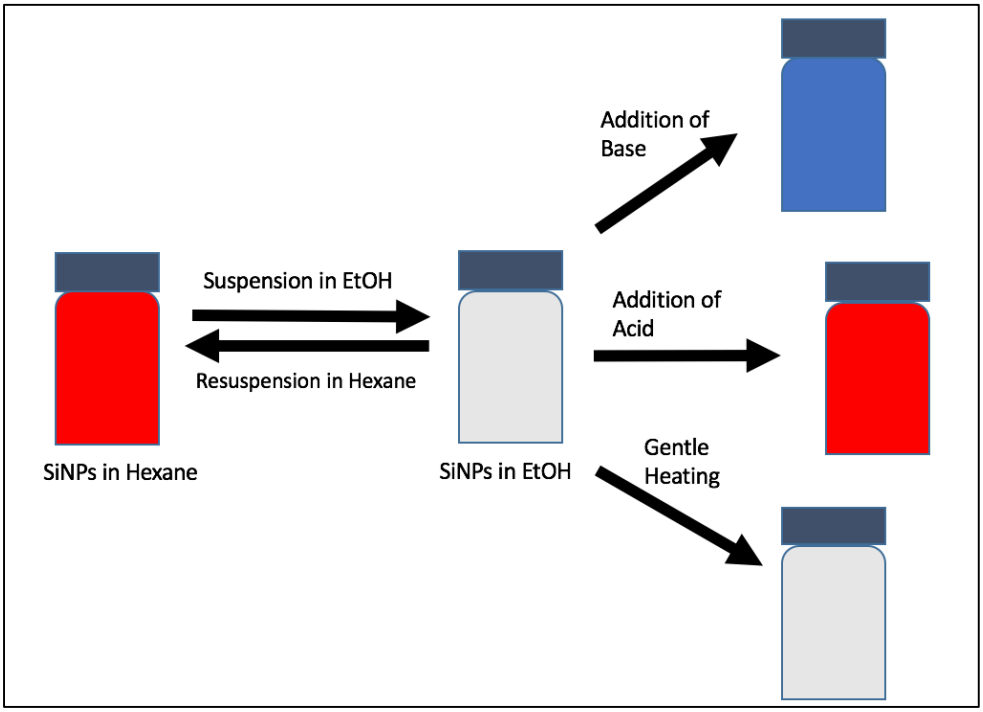


Figure 6: Reaction scheme overview for the SiNP modifications conducted.

*2.4 Characterization of SiNPs:*

PL and PLE spectroscopy were taken over the next several weeks. Measurements were taken immediately after suspension in hexane and ethanol, followed by intervals of 1 hour, 1 day, 2 days, 1 week and 2 weeks. Before each measurement, the samples were sonicated for 5 s and then added to a 1.5 mL quartz cuvette. PL measurements were taken with a 365 nm excitation wavelength, while PLE measurements were was taken at emission wavelengths of 435 and 600 nm. IR measurements were taken after the PL and PLE measurements had been concluded, 2 weeks after the initial suspension in ethanol had occurred. Concentrated SiNP samples were dropcasted onto the ATR window and IR measurements were made once the sample had completely dried.

Results and Discussion:

*3.1 Prior Work and Expected Results*

Previous research conducted in the laboratory by a predecessor produced particular outcomes for acid and base modification of SiNP suspensions, and these results were anticipated to be observed herein as well. It was previously noted that suspension of SiNPs in hexane led to stable red emissions that persisted without noticeable degradation. Transferring these SiNPs to ethanol resulted in an immediate quenching of PL. Addition of acid to this suspension was observed to cause a resurgence in red emissions almost immediately but with less intensity than those previously observed in hexane. Finally, titration with base was noted to cause the development of blue emissions after approximately 2 weeks.[35] The research herein was conducted in an attempt to provide a more detailed description of these phenomena, as well as a

comprehensive analysis of the surface chemistry of the SiNPs to determine the chemical origins of any changes in PL emissions.

*3.2 Characterization of H-SiNPs suspended in hexane:*

Prior to suspension in EtOH, the SiNP/hexane suspensions were characterized with PL/PLE and IR measurements. Upon suspension of the SiNPs in the hexane following HF etching, the samples fluoresced a strong red color. The PL spectrum for a typical colloid shows a broad, intense peak centered at ~630 nm (Figure 7).

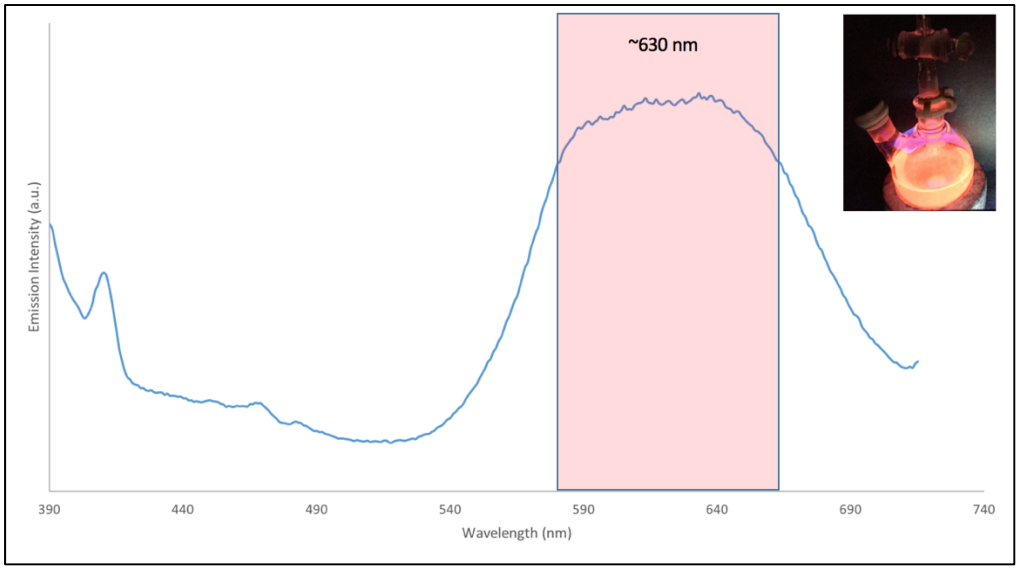


Figure 7: Photoluminescent emission spectrum for SiNPs suspended in hexane, measured immediately after suspension. The large broad peak centered at 630 nm is characteristic of this sample.

The PL from H-SiNPs has previously been reported to result from recombination across the indirect band gap, and is believed to be in good agreement with the QCE.[8] Examination of the IR spectrum reveals strong peaks present at approximately 2100 $cm^{-1}$, 900 $cm^{-1}$, and 600 $cm^{-1}$ (Figure 8). These are all indicative of Si-H stretching, which is expected immediately following

HF etching. A small peak at 1050 $cm^{-1}$ indicates siloxane bonding, indicating some non-uniformity on the SiNP surface, possibly due to some surface oxidation from air exposure.

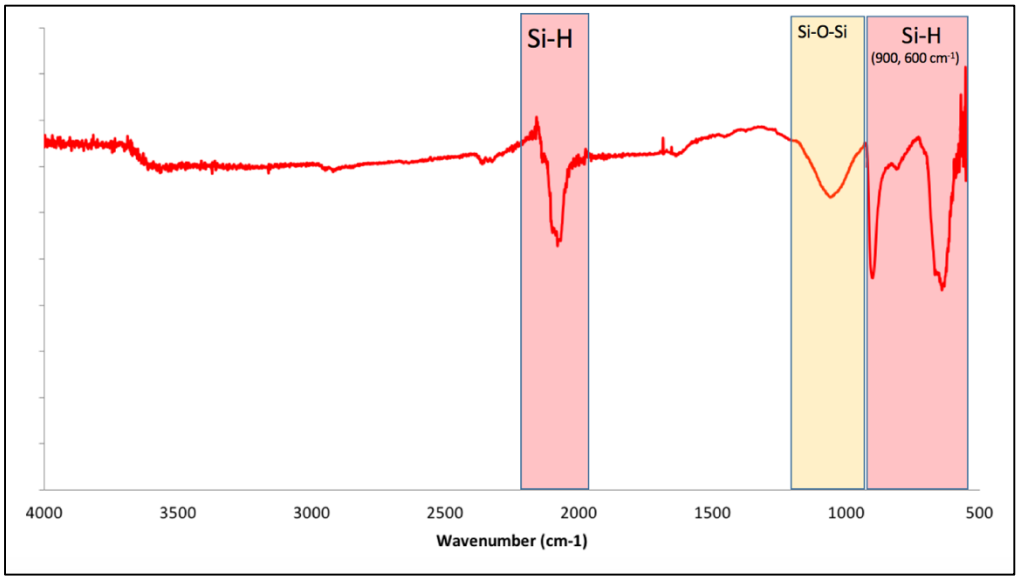


Figure 8: IR spectrum for SiNP samples suspended in hexane. Note the strong Si-H peaks at 2100, 900 and 600 $cm^{-1}$.

*3.3 Characterization of SiNPs in ethanol suspension:*

Upon suspension in EtOH, immediate quenching of the 630 nm emission was noted, as shown in Figure 9 (digital image shown in Figure 16). Additionally, a much less intense emission at 575 nm was present initially, and slowly diminished in intensity over the subsequent two weeks.

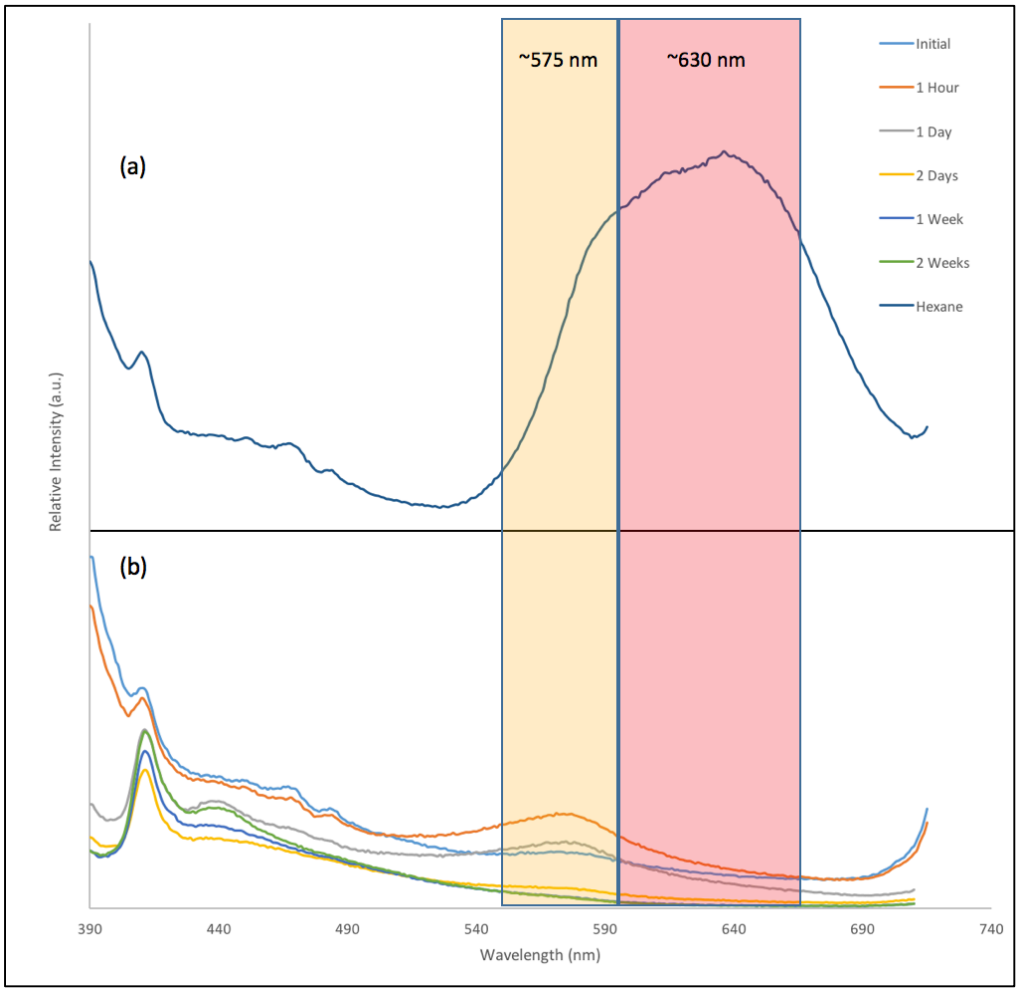


Figure 9: PL Spectra for SiNP suspensions in hexane (a) and ethanol (b). Note the shifted wavelength of the peak emission from 630 nm to 575 nm.

The IR spectra reveal structural differences between the EtOH/SiNP and hexane/SiNP suspensions (Figure 10). The Si-H peaks at 2100 $cm^{-1}$, 900 $cm^{-1}$ and 600 $cm^{-1}$ previously seen in hexane are all absent, suggesting a lack of hydrogen termination on the surface. A very strong Si-OH peak also exists at ~800 $cm^{-1}$ in the EtOH sample, as well as a greatly exaggerated peak at 1050 $cm^{-1}$ indicating Si-O-Si stretching. Both of these peaks are strong indicators of surface oxidation, which is supported by the blue shifted, quenched emissions. However, a characteristic peak at ~2900 $cm^{-1}$ seems to suggest the presence of alkyl bonding in the sample. This is reaffirmed

by a small peak at approximately 1260 $cm^{-1}$, indicating Si-C bonding. This reveals that interactions between the SiNPs and the solvent may be taking place.

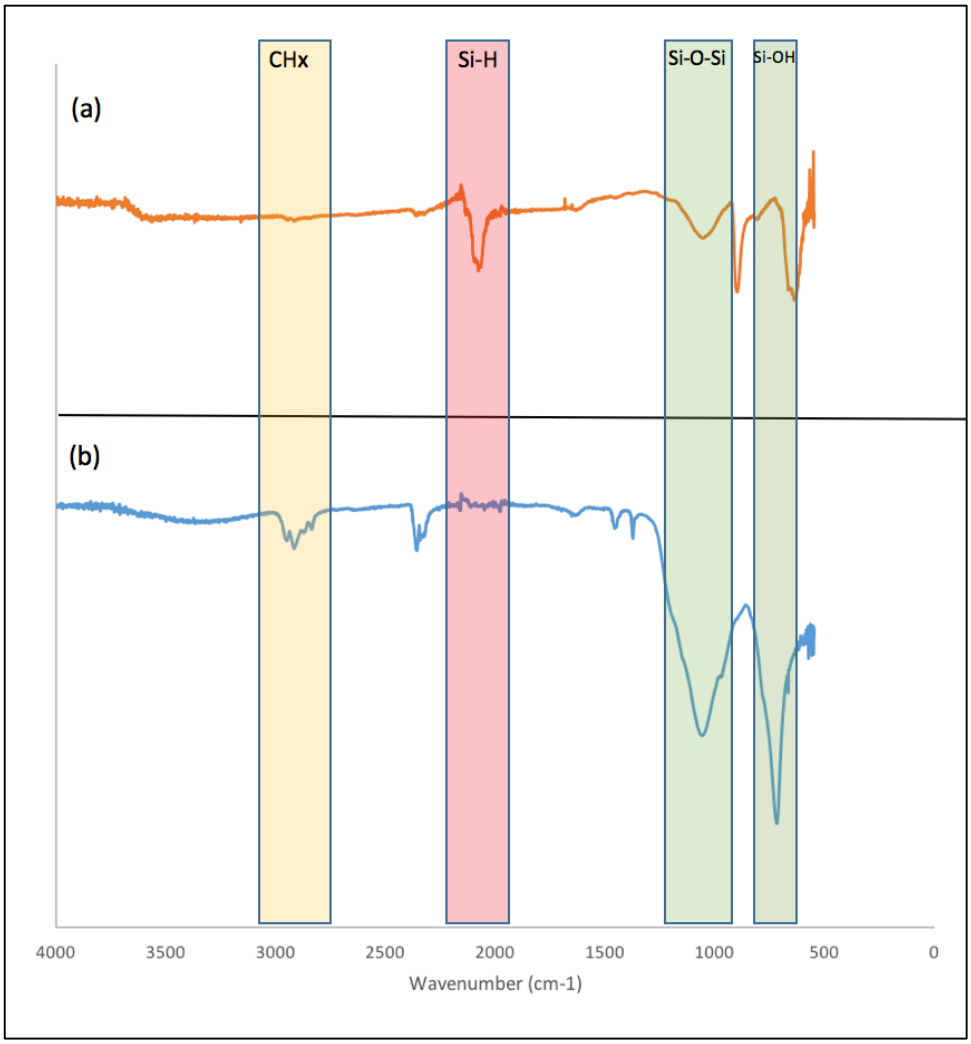


Figure 10: IR spectra for SiNPs suspended in hexane (a) and ethanol (b).

While the mechanism behind these interactions is not known, the loss of surface passivation may have resulted in the formation of reactive silicon radicals, which possess the potential to interact with the electronegative oxygen of the ethanol.[36] Additionally, the presence of a small peak at ~2400 $cm^{-1}$ in the SiNP/EtOH suspension is indicative of $CO_2$ adsorption. While this may be present due to an incomplete background subtraction, its persistence among all

SiNP/EtOH samples (Figure 12) may be the result of interactions between atmospheric $CO_2$ and the surface of the SiNP, which could also be achieved through interaction with a silicon radical.

Physical observation of the sample showed that the SiNP/hexane suspension appeared opaque and muddy, and possessed a brown-yellow color. Over time, the SiNPs aggregated on the bottom of the flask in a web-like, stringy pattern. Upon being transferred to ethanol, the suspensions initially retained the muddy appearance and brown-yellow color, but this gradually subsided over time, until the solutions appeared translucent. Aggregations of particles at the bottom of the flask lacked the thick stringy pattern, but rather, featured more of a fine, particulate appearance.

*3.4 Characterization of SiNPs following acid/base additions:*

Titration of the SiNP/EtOH sample with acid resulted in the gradual resurgence of emissions, beginning with the time of the acid addition, at which point the emissions appeared quenched (digital image shown in Figure 16). The intensity then increased, with noticeable PL present after 1 hour (Figure 11). These emissions reached maximum intensity after approximately 1 day, and began to subside in intensity thereafter. After a week, emissions were greatly diminished. The peak emission wavelength persisted at 575 nm, but in sharp contrast to the unmodified ethanol suspension, a resurgence of emissions was seen almost rivaling the hexane/SiNP suspension in intensity.

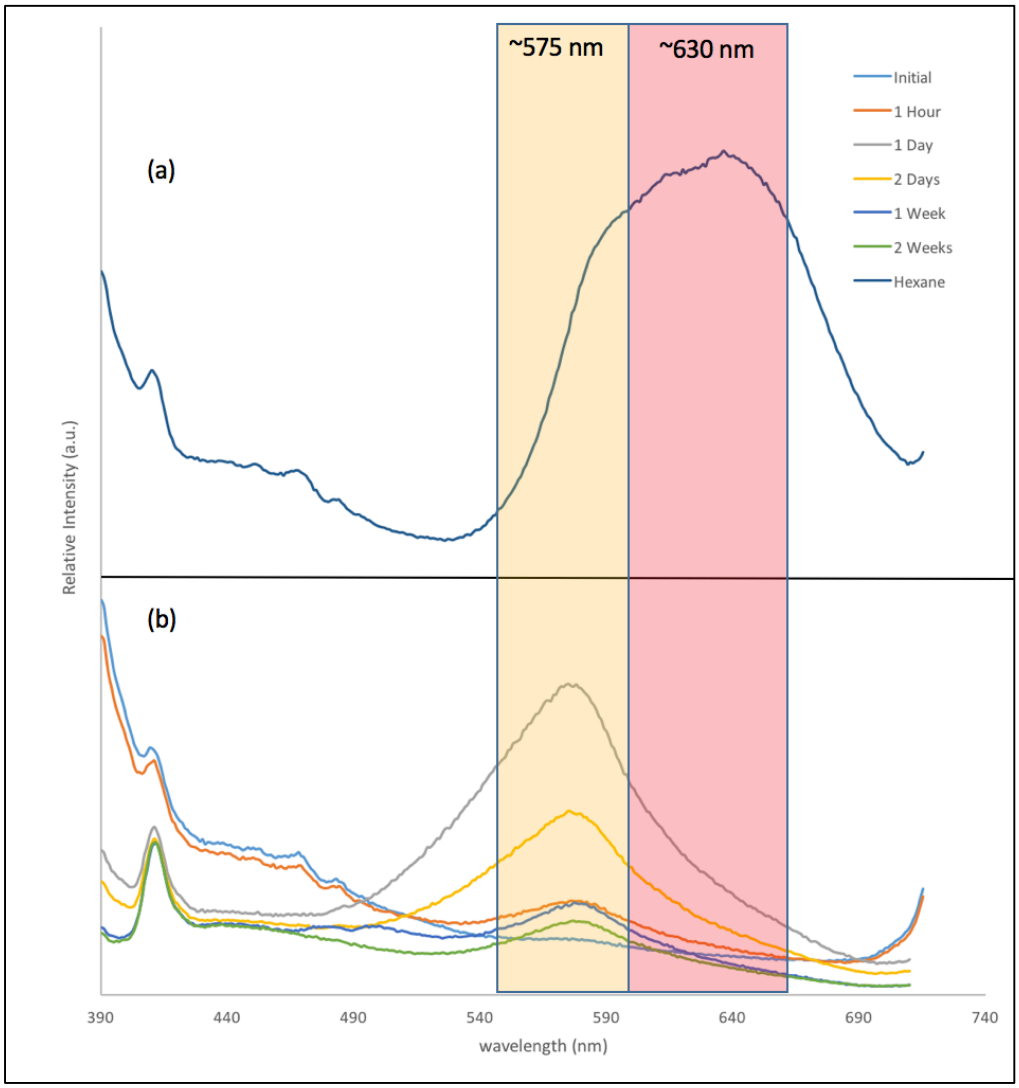


Figure 11: PL spectra for SiNPs suspended in hexane (a) and EtOH titrated with acid (b). Notice the shifting of the peak wavelength, and large intensity of the acid modified sample.

The structural differences in the SiNPs may indicate the mechanism of this phenomenon. First, the Si-OH peak seen in the EtOH/SiNP suspension is notably absent from the acid modified sample, along with a slightly reduced Si-O-Si peak at 1050 $cm^{-1}$ (Figure 12). This may indicate that the acid may have eliminated some of the surface oxidation that had previously developed upon suspension in EtOH. However, the Si-H peaks present at 2100 $cm^{-1}$, 900 $cm^{-1}$, and 600 $cm^{-1}$ are still absent. This shows that the acid did not re-passivate the surface. Additionally, the alkyl

peak seen in the EtOH sample at 2900 $cm^{-1}$ is absent, and the Si-C peak at 1260 $cm^{-1}$ is noticeably diminished.

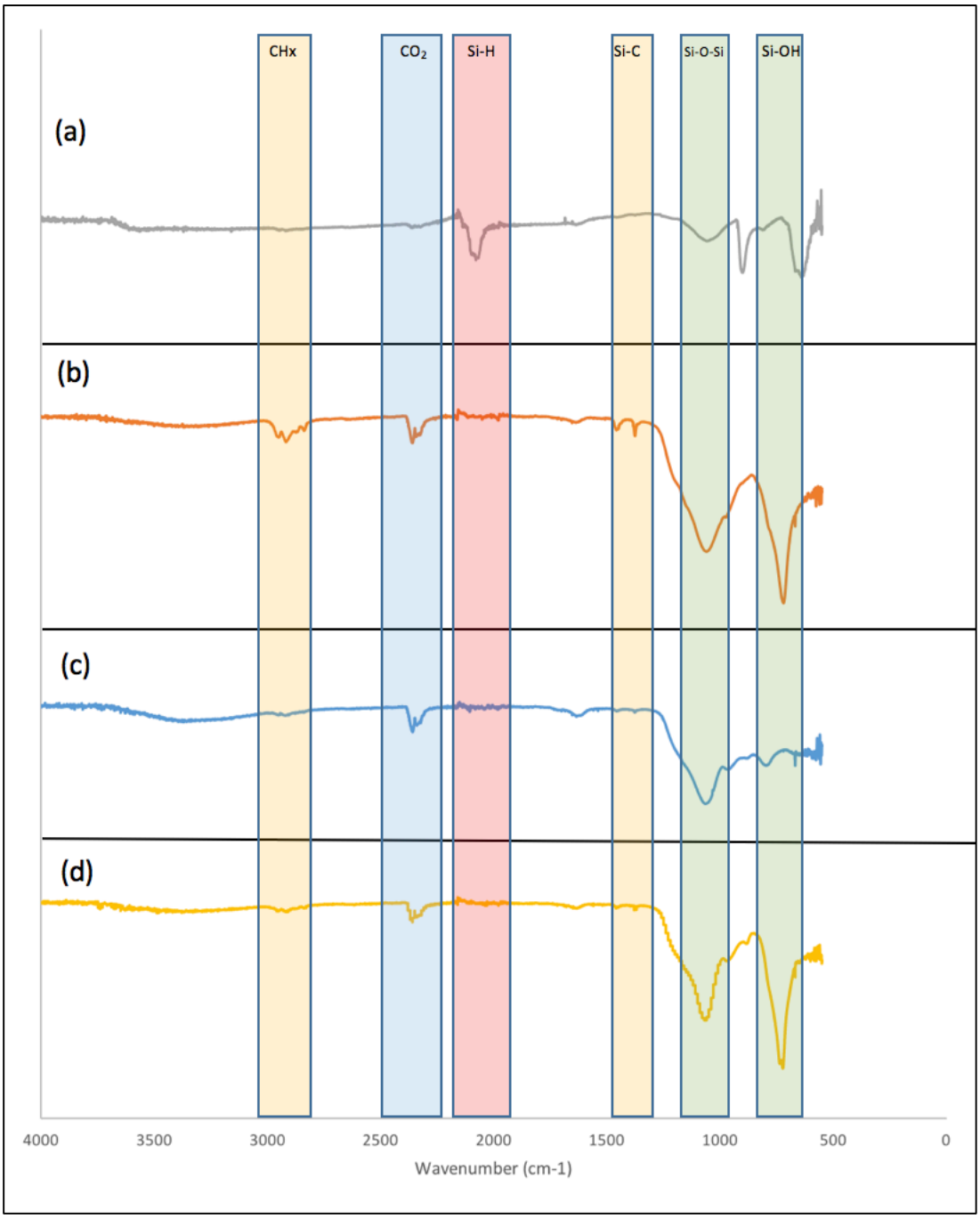


Figure 12: IR spectra for SiNPs suspended in hexane (a), EtOH (b), acid modified EtOH (c), and base modified EtOH (d).

The presence of blue shifted emissions in the SiNPs and the lack of evidence for hydrogen passivation strongly suggests that a different mechanism may be responsible for the red PL, in light of the literature consensus regarding the role of surface passivation in SiNP PL. First, it is possible that the SiNP emissions are in good agreement with those predicted by the QCE; if this is the case, then the nanoparticles must have been etched further by the acid-treated ethanolic suspension, as this would result in a smaller particle size and therefore a shorter emission wavelength. However, if such etching did occur, it cannot have resulted in the passivation of the surface with hydrogen, due to the lack of corresponding peaks on the IR. If the emissions are not in agreement with the QCE model, this may be indicative of functional groups on the surface that impact the radiative mechanism of PL. Given the peaks on the IR however, this can not be due to surface oxidation alone, as Si-OH and Si-O-Si stretching present on the EtOH spectrum had a quenching effect. Discrepancies among the fingerprint region may be indicative of the functional groups responsible for such emissions. Determination of whether these SiNPs are in agreement with QCE may be determined after evaluating the size with DLS or TEM both before and after suspension, to determine differences (if any) in the particle size, and should be the subject of a future study.

For titration of the sample with base, it was anticipated beforehand that the SiNPs would fluoresce blue approximately 2 weeks following titration with base. However, this did not occur, and little change was observed between the unmodified ethanol and the base-modified suspension. No identifiable emission intensity was observed on the PL spectrum (Figure 13).

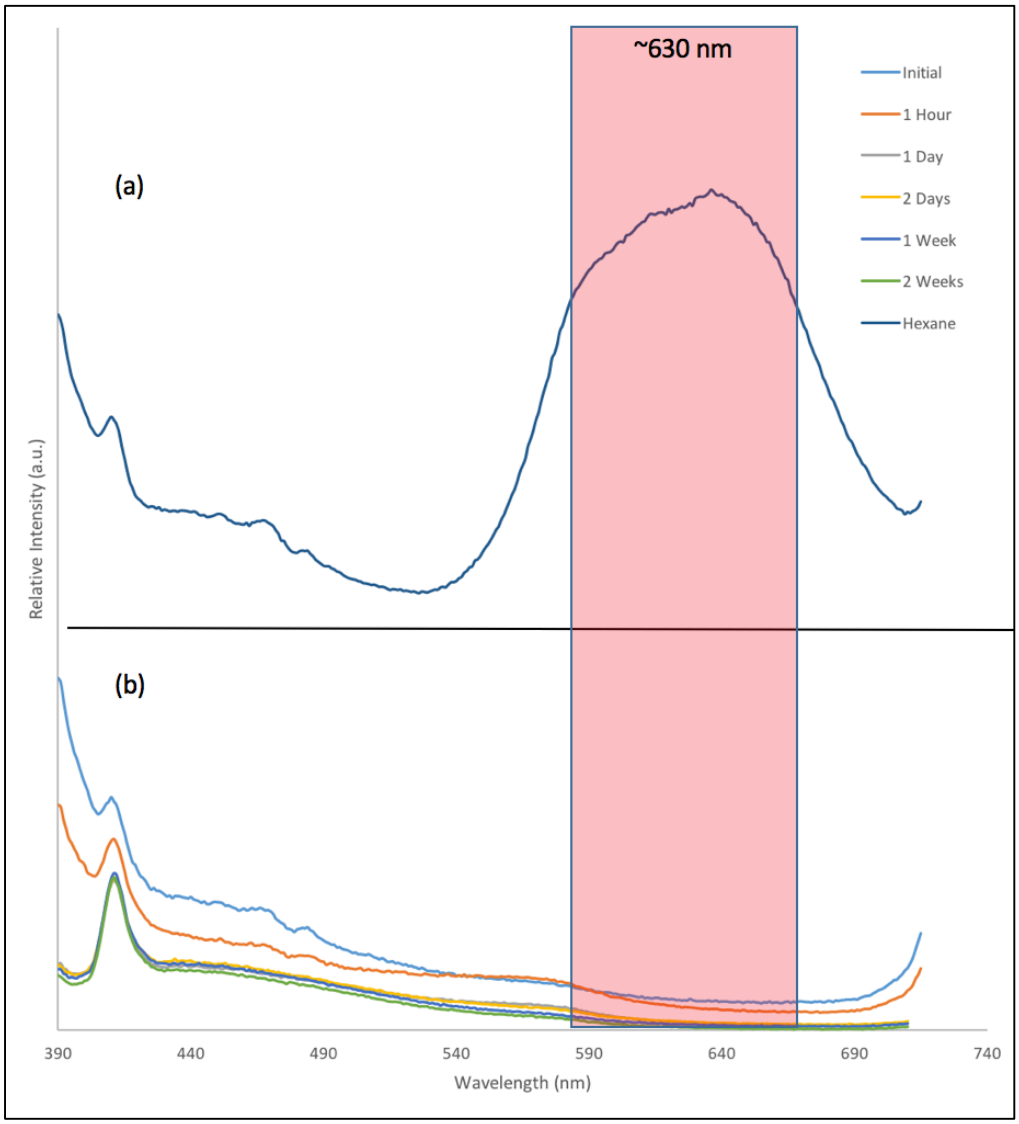


Figure 13: PL spectra for SiNPs suspended in hexane (a), and base-modified EtOH (b).

The IR spectrum for the base treated ethanol suspension reveals the lack of the alkyl bonding peak at 2900 $cm^{-1}$ previously seen in the EtOH/SiNP suspension, as well the disappearance of the Si-C peak at 1260 $cm^{-1}$; however, no other changes exist (Figure 12). Large peaks are still present at 1050 $cm^{-1}$ and 810 $cm^{-1}$, indicating Si-O-Si and Si-OH stretching, and the fingerprint regions of both spectra appear largely identical. From this, the exact impact of the base on the structure of the SiNPs is relatively unknown. While it appears to have reduced the

interactions between the base and solvent due to the lack of alkyl stretches, it did not diminish the degree of surface oxidation present on the SiNPs. However, there are some indications that the presence of base is detrimental to the structure of the SiNPs, as prior testing with more concentrated base additions resulted in the formation of bubbles and an almost instantaneous change in the color and opacity of the suspension. When a larger amount of base was added to the sample, the solutions gently fizzed for several seconds. The sample, which initially appeared muddy, became clear, and over time, became translucent, which suggested the complete dissolution of the H-SiNPs (Figure 14).

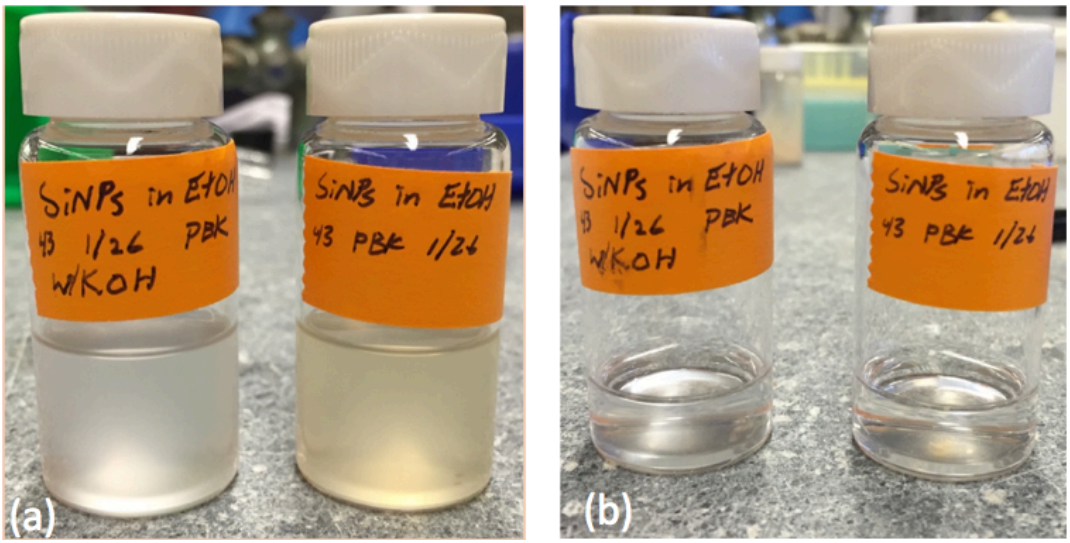


Figure 14: SiNP suspensions in ethanol with (left) and without (right) treatment with base. (a) Both samples immediately after suspension in ethanol and treatment with base. (b) Both samples 2 days after suspension and treatment.

*3.5 Blue Emissions in Base-Modified EtOH*

One particular aliquot of ethanol treated with base generated stable blue emissions immediately after titration; however, this was not a reproducible result. Upon addition and sonication, the sample fluoresced a faint blue-green color. The PL spectrum for the SiNPs in base resulted in a fairly intense peak centered at approximately 485 nm, representing these emissions.

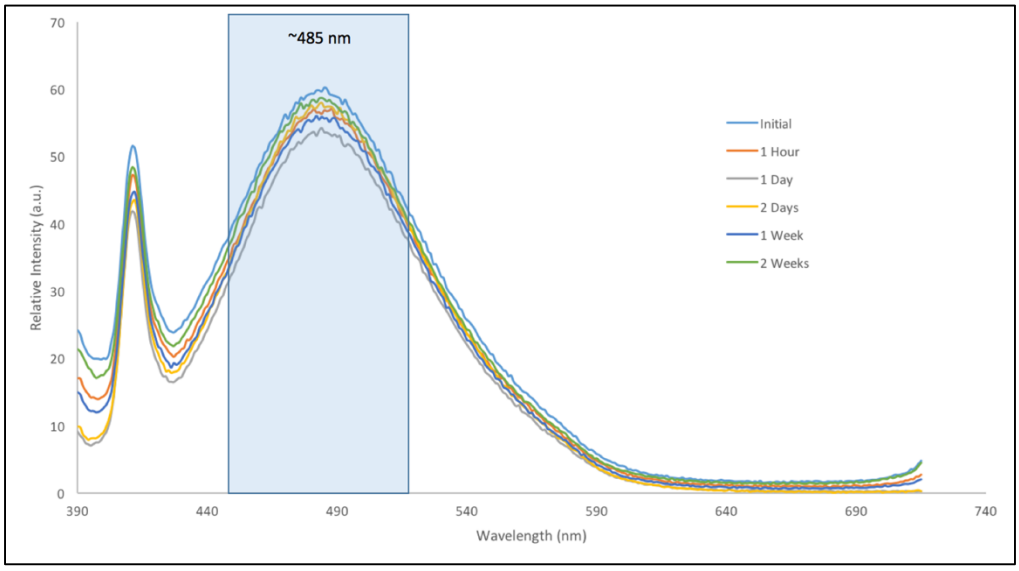


Figure 15: PL spectrum for SiNPs suspended in base-modified EtOH. The large peak present on this spectrum at 485 nm was present in other base modified samples using the same set of SiNPs, but was not reproducible among other sets.

This peak was present among all base-modified samples from the same extracted set of nanoparticles (Figure 15). However, it was not reproducible among other sets. This seems to indicate a systematic error with the production of the SiNPs used in that set, which may have resulted from issues with the anneal or etch. Previously, it was found that the position of the alumina boat used for the annealing process in the tube furnace had an impact on the heat distribution of temperature of the polymer, and led to an annealed product that varied in consistency and appearance from other sets. Additionally, some errors were occasionally reported

with the etching process, as the etched nanoparticles would remain in the aqueous layer after agitation. While the source of these issues is not entirely clear, it is possible that such discrepancies in the consistency of the SiNP batches may be the source of the blue shifted peak.

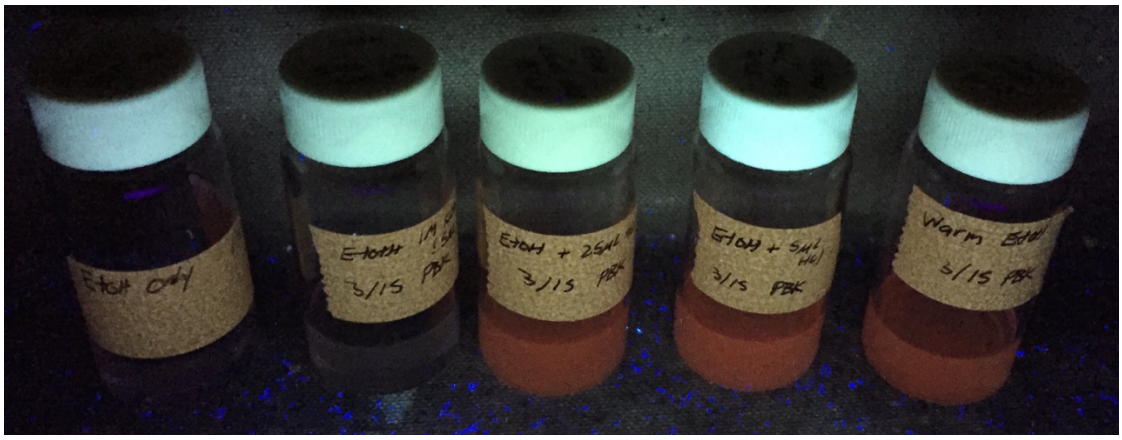


Figure 16: SiNP suspensions following modification. The SiNP suspensions, from left to right: unmodified EtOH, EtOH treated with 5 µL KOH, EtOH treated with 25 µL of HCl, EtOH treated with 5 µL of HCl, warmed EtOH. Notice the PL present in the three right samples.

*3.6 Further Characterization of SiNPs in EtOH*

To further investigate the quenching properties of EtOH, the SiNP/EtOH suspension was characterized after heating, as well as following resuspension of the SiNPs in hexane in an attempt to restore emissions. Heating of the EtOH/SiNP mixture was performed immediately upon suspension, at which point the sample was gently heated in a warm water bath to $60^0$C. This temperature was held constant for 30 minutes, at which point PL and PLE measurements were taken. It was observed that heating of the sample resulted in a resurgence of emissions at 575 nm (Figure 17). Emissions were present immediately after heating had ceased, and reached maximum intensity after 1 hour, after which they began to subside. Weak emissions were present after 1 day, but none persisted thereafter.

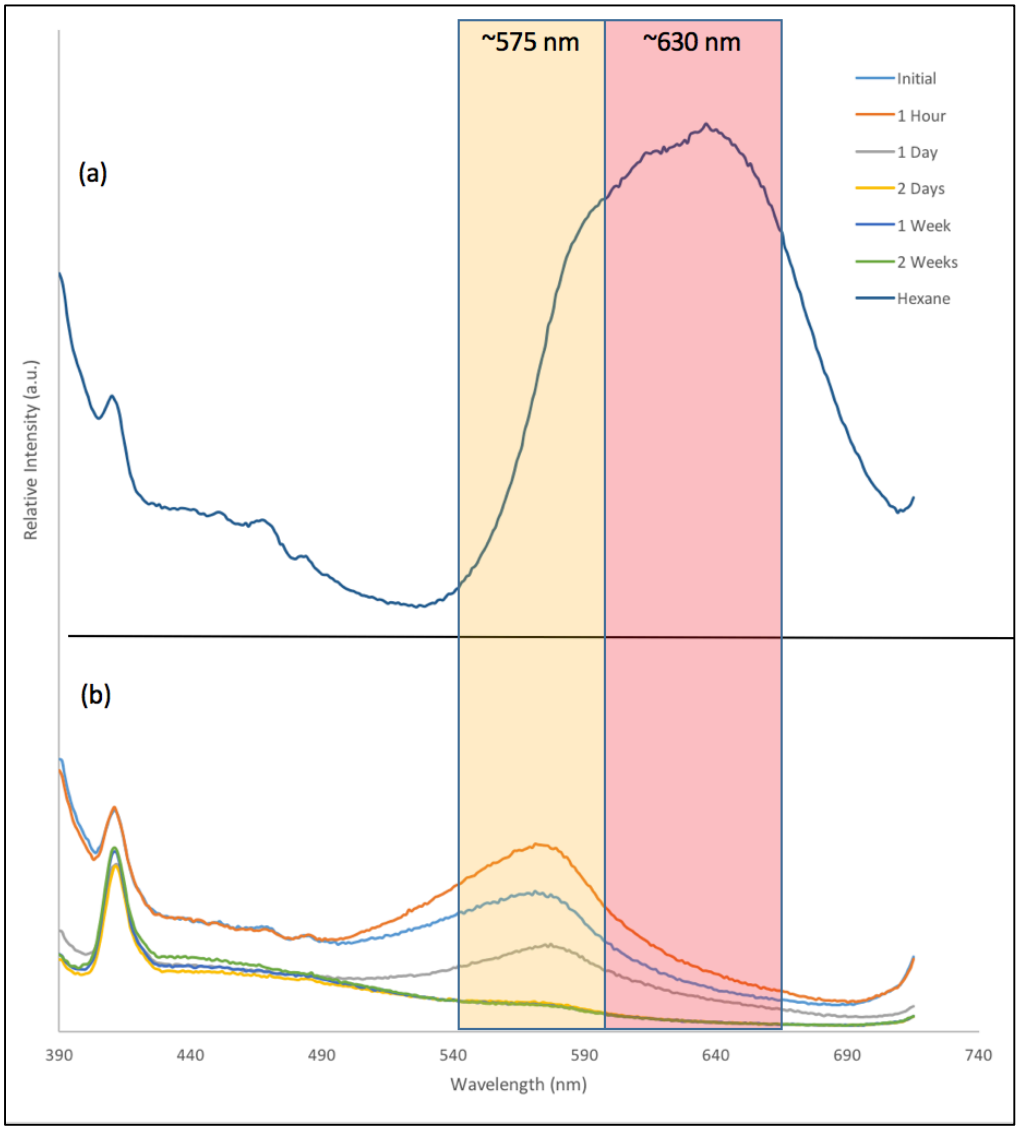


Figure 17: PL spectra for SiNPs suspended in hexane (a), and warmed EtOH (b).

Resuspension of SiNPs in hexane following their suspension in EtOH was accomplished through centrifugation of the SiNP/EtOH samples 5 minutes after suspension, followed by replacement of the ethanol with an equivalent volume of hexane. Observation of the sample resuspended in hexane revealed red fluorescence, but but with a greatly diminished intensity in comparison to the SiNPs originally in hexane. The sample also notably retained its muddy brown-

yellow complexion. However, after only several minutes, the red emissions completely vanished, and no longer fluoresced at all under UV light.

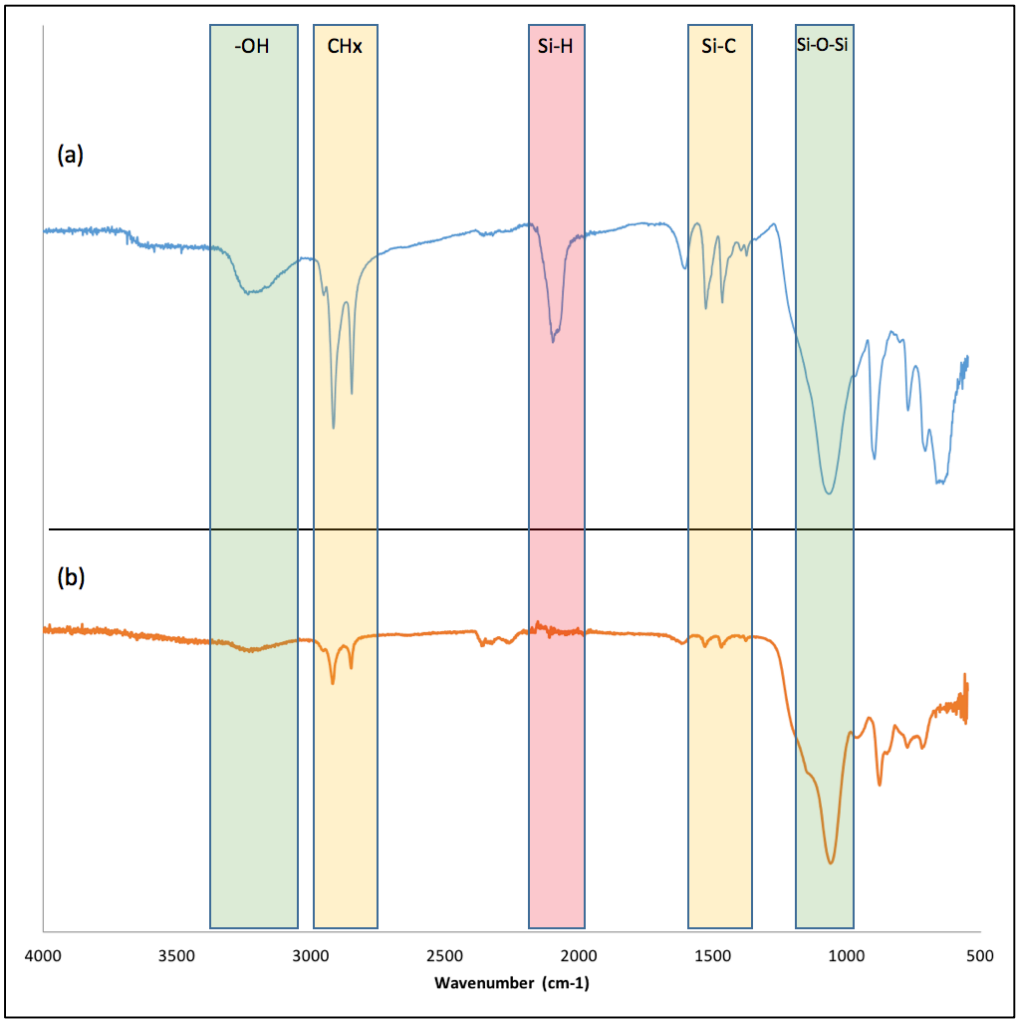


Figure 18: IR spectra for SiNPs suspended in hexane (a) and resuspended in hexane following suspension in ethanol (b). Note, measurements were taken on a hexane sample several weeks after extraction.

While the IR spectra of both samples were taken immediately following resuspension, the SiNP/hexane suspension was several weeks old, and interesting and uncharacteristic peaks were present on the IR spectrum. An –OH peak at about 3200 $cm^{-1}$ and an unusually prominent siloxane peak at 1050 $cm^{-1}$ are both present, as well as strong alkyl peaks at 2900 $cm^{-1}$ and a Si-C peak at

1260 $cm^{-1}$. This may indicate some form of interaction between the SiNPs and the hexane solvent. However, despite these structural deviations, the sample still fluoresced red, and the presence of surface passivation is reflected on the IR with an Si-H peak at 2100 $cm^{-1}$. Interestingly, the IR spectrum of the sample resuspended in hexane following suspension in ethanol shares many similarities with that of the hexane sample; both possess alkyl peaks, Si-C peaks and siloxane peaks, albeit all are greatly diminished. However, two notable differences are the absence of a –OH peak, and the disappearance of the Si-H peak. This observation suggests a removal of the hydrogen terminated surface by the ethanol that is not restored upon resuspension in an organic solvent. This result raises questions for future investigation.

## Conclusion:

Throughout this research, a number of observations were made regarding the behavior of SiNPs upon suspension in various media. While in hexane, the SiNPs fluoresced red with a peak emission wavelength of 630 nm, which was an expected outcome. This may be due to a hydrogen passivated surface resulting in a particle with emissions consistent with those predicted by QC. Suspension in ethanol resulted in an immediate quenching of PL emissions, as well as a shift of the peak emission wavelength from 630 nm in hexane to 575 nm. The IR spectrum indicates the presence of hydroxyl groups, siloxane bonding and alkyl stretching, and this in turn may hint at a possible mechanism behind the quenched and shifted emissions. Titration of the sample with HCl resulted in a similar shift in emission wavelength, but a resurgence in emission intensity, peaking after 1 day. The IR spectrum for this sample indicated a reduction in the Si-OH peak, but no subsequent surface passivation, leaving questions as to the mechanistic origin for the resultant PL emissions. Finally, while blue emissions were expected, addition of base to the SiNP/EtOH

suspension led to no resurgence of emissions while the IR revealed no major differences between the base treated sample and the unmodified EtOH sample.

Further modification to the ethanol suspension revealed interesting SiNP behavior. This included a resurgence of emissions of the sample when heated that peaked after an hour, then subsided thereafter. Additionally, resuspension of the SiNP samples into hexane yielded a restoration of PL, which quickly abated. These observations all highlight the complexity of the interactions between the SiNPs and the ethanol solvent, as well as the unique impact that both acidic and basic media have on the characteristics and properties of these particles. While the focus of this work is narrow in scope, the implications of the observations may spurn future work in the field to investigate these phenomena and uncover the mechanisms by which the PL emissions are generated by the SiNPs.

Future Work:

Future work in this field may involve refining the processes utilized in this research, as well as using different spectroscopic methods for a more thorough characterization. The use of IR in this study was incredibly revealing as to the structure of the SiNPs. However, there are inherent problems with the IR spectra. Since the quantity of SiNPs in ethanol was quite small, and recovery of the sample after IR spectroscopy is very difficult, the IR was taken after the conclusion of the PL/PLE data collection. This means that *initial* modifications to the SiNPs by the acid, base and ethanol would not be recorded, due to the IR data being collected approximately 2 weeks following initial suspension in ethanol. Also, the incredibly small amount of SiNPs present in each aliquot meant that the IR spectra are flat and featureless compared to that of larger, more abundant samples. To assuage this problem, future research may invoke the reservation of samples for IR

that may be taken early on, to understand the immediate impact of EtOH suspension and sample modification.

Future studies in this area may also evoke the use of TEM and DLS as tools to assess the sizes of the nanoparticles. Originally, nanoparticle size was not a major point of consideration, given the focus on the presence of functional groups and surface oxidation on the SiNP surface. However, there is a possibility of further etching by the HCl solution, which may be responsible for the unique resurgence in emissions. Additionally, the possibility of non-uniformity between etches may also necessitate the use of such spectroscopic tools. Using DLS and TEM to determine the SiNP sizes both before and after the sample modification would be useful, not only to assess the reliability of the etching process to produce NPs of consistent size, but also to determine if the SiNP sizes are altered by the acid or base solution, and if this is responsible for the change in wavelength and intensity of emissions. The use of these tools can also provide images of the SiNP surface, which in turn may reveal the presence of functional groups, oxide layers, or surface patterns.

References:

[1] Heiligtag, F. J.; Niederberger, M. The fascinating world of nanoparticle research *Mat. Today* **2013**, 16, 262-271

[2] Huan, C.; Shu-Qing, S. Silicon nanoparticles: Preparation, properties and applications *Chin. Phys. B.* **2014**, 23, 1-14

[3] Veinot, J. G. C. Synthesis, surface functionalization, and properties of freestanding silicon nanocrystals *Chem. Commun.* **2006**, 4160-4168

[4] Hughes, B. K.; Luther, J. M.; Beard, M. C. The Subtle Chemistry of Colloidal, Quantum-Confined Semiconductor Nanostructures *Acs Nano*. **2012**, 6, 4573-4579

[5] Alivisatos, A. P. Perspectives on the Physical Chemistry of Semiconductor Nanocrystals *J. Phys. Chem.* **1996**, 100, 13226-13239

[6] Wolf, O.; Dasog, M.; Yang, Z.; Balberg, I.; Veinot, J. G. C.; Millo, O.; Doping and Quantum Confinement Effects in Single Si Nanocrystals Observed by Scanning Tunneling Spectroscopy Nano Lett. **2013**, 13, 2516-2521

[7] Chen, F.; Ramayya, E. B.; Euaruksakul, C.; Himpsel, F. J.; Celler, G. K.; Ding, B.; Knezevic, I.; Lagally, M. G. Quantum Confinement, Surface Roughness, and the Conduction Band Structure of Ultrathin Silicon Membranes *Acs Nano* **2010**, 4, 2466-2474

[8] Luo, J.; Franceschetti, A.; Zunger, A. Direct-Bandgap InAs Quantum Dots have Long-Range Electron-Hole Exchange whereas Indirect Gap Si Dots have Short-Range Exchange *Nano Lett.* **2009**, 9, 2648-2653

[9] Chukwoucha, E. O.; Onyeaju, M. C.; Harry, T. S. T. Theoretical Studies on the Effect of Confinement on Quantum Dots Using the Brus Equation *Wrld. J. Cnd. Mtr. Phys.* **2012**, 2, 96-100

[10] Wang, Q.; Seo, D. Synthesis of Deep-Red-Emitting CdSe Quantum Dots and General Non-Inverse Square Behavior of Quantum Confinement in CdSe Quantum Dots *Chem. Mater.* **2006**, 18, 5764-5767

[11] Fuzell, J.; Thibert, A.; Atkins, T. M.; Dasog, M.; Busby, E.; Veinot, J. G. C.; Kauzlarich, S. M.; Larsen, D. S. Red States versus Blue States in Colloidal Silicon Nanocrystals: Exciton Sequestration into Low-Density Traps *J. Phys. Chem. Lett.* **2013**, 4, 3806-3812

[12] Hua, F.; Erogbogbo, F.; Swihart, M. T.; Ruckenstein, E. Organically Capped Silicon Nanoparticles with Blue Photoluminescence Prepared by Hydrosilylation Followed by Oxidation *Langmuir* **2006**, 22, 4363-4370

[13] Li, S.; Silvers, S. J.; El-Shall, M. S. Surface Oxidation and Luminescence Properties of Weblike Agglomeration of Silicon Nanocrystals Produced by a Laser Vaporization-Controlled

Condensation Technique *J*. *Phys*. *Chem*. *B* **1997**, 101, 1794-1802

[14] Wilson, W. L.; Szajowski, P. F.; Brus, L. E.; Quantum Confinement in Size-Selected, Surface-Oxidized Silicon Nanocrystals *Science*, **1993**, 262, 1242-1244

[15] Dasog, M.; De los Reyes, G. B.; Titova, L. V.; Hegmann, F. A.; Veinot, J. G. C.; Size vs. Surface: Tuning the Photoluminescence of Freestanding Silicon Nanocrystals Across the Visible Spectrum via Surface Groups *Acs Nano* **2014**, 8, 9636-9648

[16] Knittel, F.; Gravel, E.; Cassette, E.; Pons, T.; Pillon, F. Dubertret, B.; Doris, E. On the Characterization of the Surface Chemistry of Quantum Dots *Nano Lett*. **2013**, 13, 5075-5078

[17] Yang, Z.; De los Reyes, G. B.; Titova, L. V.; Sychugov, I.; Dasog, M.; Linnros, J.; Hegmann, F. A.; Veinot, J. G. C. Evolution of the Ultrafast Photoluminescence of Colloidal Silicon Nanocrystals with Changing Surface Chemistry *Acs photonics* **2015**, 2, 595-605

[18] Inerbaev, T. M.; Masunov, A. E.; Khondaker, S. I.; Dobrinescu, A.; Plamada, A.; Kawazoe, Y. Quantum chemistry of quantum dots: Effects of ligands and oxidation *J*. *Chem*. *Phys*. **2009**, 131, 1-7

[19] Dasog, M.; Yang, Z.; Regli, S.; Atkins, T. M.; Faramus, A.; Singh, M. P.; Muthuswarmy, E.; Kauzlarich, S. M.; Tilley, R. D.; Veinot, J. G. C. Chemical Insight into the Origin of Red and Blue Photoluminescence Arising from Freestanding Silicon Nanocrystals *Acs Nano* **2013,** 7, 2676-2685

[20] Nishida, M.; Electronic Structure of Silicon Quantum Dots: Calculations of Energy-Gap Redshifts Due to Oxidation *J*. *Appl*. *Phys*. **2005**, 98, 1-6

[21] Vasiliev, I.; Chelikowsky, J. R.; Martin, R. M. Surface oxidation effects on the optical properties of silicon nanocrystals *Phys*. *Rev*. *B* **2002**, 65, 1-4

[22] Wolkin, M. V.; Jorne, J.; Fauchet, P. M. Electronic States and Luminescence in Porous Silicon Quantum Dots: The Role of Oxygen *Phys*. *Rev*. *Lett*. **1999**, 82, 197-200

[23] Zeng, Y.; Chen, L.; Liu, G.; Xu, H.; Song, W. Insight into the effects of surface oxidation and carbonization on the electronic properties of silicon quantum dots and silicon slabs: a density functional study *RSC Adv.* **2014**, 4, 60948-60952

[24] Chiu, S.; Manhat, B. A.; DeBenedetti, W. J. I.; Brown, A. L.; Fichter, K.; Vu, T.; Eastman, M.; Jiao, J.; Goforth, A. M. Aqueous red-emitting silicon nanoparticles for cellular imaging: Consequences of protecting against surface passivation by hydroxide and water for stable red emission *J. Mater. Res.* **2013**, 28, 216-230

[25] O'Farrell, N.; Houlton, A.; Horrocks, B. R. Silicon nanoparticles: applications in cell biology and medicine *Int. Journal Nanomed.* **2006**, 1, 451-472

[26] Hardman, R. A Toxicological Review of Quantum Dots: Toxicity Depends on Physicochemical and Environmental Factors *Env. Hlth. Per.* **2006**, 114, 165-172

[27] Henderson, E. J.; Kelly, J. A.; Veinot, J. G. C. Influence of $HSiO_{1.5}$ Sol-Gel Polymer Structure and Composition on the Size and Luminescent Properties of Silicon Nanocrystals *Chem. Mater.***2009**, 21, 5426-5434

[28] Hessel, C. M.; Henderson, E. J.; Veinot, J. G. C. Hydrogen Silsesquioxane: A Molecular Precursor for Nanocrystalline Si-$SiO_2$ Composites and Freestanding Hydride-Surface-Terminated Silicon Nanoparticles *Chem. Mater.* **2006**, 18, 6139-6146

[29] Hessel, C. M.; Henderson, E .J.; Veinot, J. G. C. An Investigation of the Formation and Growth of Oxide-Embedded Silicon Nanocrystals in Hydrogen Silsesquioxane-Derived Nanocomposites *J. Phys. Chem. C* **2007**, 111, 6956-6961

[30] Liao, Y.; Nineow, A. M.; Roberts, J. T. Surface Chemistry of Aerosolized Nanoparticles: Thermal Oxidation of Silicon *J. Phys. Chem. B* **2006**, 110, 6190-6197

[31] Kang, J. J.; Musgrave, C. B. The mechanism of $HF/H_2O$ chemical etching of $SiO_2$ *J. Chem. Phys.* **2002**, 116, 275-280

[32] Pan, K.; Zhang, L.; Wang, J.; Lin, J; Chen, G. Oxygen removal from raw silicon powder by the HF-ethanol solution etching *Surf. Interfance Anal.* **2013**, 45, 955-961

[33] Hansen, U.; Vogl, P. Hydrogen passivation of silicon surfaces: A classical molecular-dynamics study *Phys. Rev. B* **1998**, 57, 295-304

[34] Nunez, J. R. R.; Kelly, J. A.; Henderson, E. J.; Veinot, J. G. C. Wavelength-Controlled Etching of Silicon Nanocrystals *Chem. Mater.* **2012**, 24, 346-352

[35] Chiu, S. Photoluminescent Silicon Nanoparticles: Fluorescent Cellular Imaging Applications and Photluminescence Behavior Study Ph.D. Dissertation, Portland State University, Portland, OR 2015

[36] Wayner, D. D. M.; Wolkow, R. A. Organic modification of hydrogen terminated silicon surfaces *J. Chem. Soc.* **2002**, 2, 23-34